General Disclaimer

One or more of the Following Statements may affect this Document

- This document has been reproduced from the best copy furnished by the organizational source. It is being released in the interest of making available as much information as possible.

- This document may contain data, which exceeds the sheet parameters. It was furnished in this condition by the organizational source and is the best copy available.

- This document may contain tone-on-tone or color graphs, charts and/or pictures, which have been reproduced in black and white.

- This document is paginated as submitted by the original source.

- Portions of this document are not fully legible due to the historical nature of some of the material. However, it is the best reproduction available from the original submission.

Produced by the NASA Center for Aerospace Information (CASI)

11176-H066-R0-00

APOLLO SPACECRAFT SYSTEMS ANALYSIS PROGRAM

TECHNICAL REPORT

TASK E-34D

NAS9-8166

4 November 1968

ANALYSIS OF RENDEZVOUS RADAR PEARL FLIGHT TEST DATA

Prepared For

NATIONAL AERONAUTICS AND SPACE ADMINISTRATION
MANNED SPACECRAFT CENTER
HOUSTON, TEXAS

FACILITY FORM 602

N69-18036
(ACCESSION NUMBER)

(THRU)

46
(PAGES)

1
(CODE)

CR 92493
(NASA CR OR TMX OR AD NUMBER)

21
(CATEGORY)

TRW
SYSTEMS GROUP

NASA CR 92493

11176-H066-R0-00

APOLLO SPACECRAFT SYSTEMS ANALYSIS PROGRAM

ANALYSIS OF RENDEZVOUS RADAR PEARL FLIGHT TEST DATA

TASK E-34D

4 November 1968

Prepared by: D. Dobby

Prepared by: M. Doty

Approved by: C. E. Blakely
Task Manager

Approved by: J. DeVillier, Manager
Communication and Sensor Systems
Department

TRW
SYSTEMS GROUP

ACKNOWLEDGEMENTS

The authors wish to acknowledge the contributions of R. E. Hughes (GAEC/WSMR), P. R. Pellette (GAEC/WSMR), and T. A. Gundlach (GAEC/WSMR) for their helpful discussions concerning the Rendezvous Radar PEARL test data.

TABLE OF CONTENTS

1.0 INTRODUCTION 1

2.0 GENERAL DISCUSSION OF RENDEZVOUS RADAR PEARL FLIGHT TESTS. . . . 2

2.1 PEARL Configuration 2

2.2 Flight Profiles 2

2.3 Parameters Measured 7

2.4 Data Analysis Procedure 7

3.0 RESULTS OF RENDEZVOUS RADAR TEST ANALYSIS. 9

3.1 Summary of Results. 9

3.2 Shaft and Trunnion. 11

3.3 Range Rate. 19

3.4 Range 21

4.0 CONCLUSIONS. 23

APPENDIX A

DERIVATION OF THE PERIOD OF SHAFT OSCILLATION DUE TO MULTIPATH. 24

APPENDIX B

DERIVATION OF THE AMPLITUDE OF SHAFT OSCILLATION DUE TO MULTIPATH. 31

APPENDIX C

APPLICATION OF MULTIPATH PHENOMENON TO LUNAR MISSION 34

APPENDIX D

SIGNAL-TO-NOISE VERSUS RANGE FOR RR/T. 36

REFERENCES. 39

LIST OF ILLUSTRATIONS

Figure		Page
2-1	Maps of X,S,L and H Profiles Flown in Rendezvous Radar WSMR Tests	3
2-2	Maps of AA,W,Z,T and Y Profiles Flown in Rendezvous Radar WSMR Tests	4
2-3	Maps of E and B Profiles Flown in Rendezvous Radar WSMR Tests	5
2-4	Map of N Profile Flown in Rendezvous Radar WSMR Tests	6
3-1	Examples of Multipath Taken From Recorded Data of the Rendezvous Radar WSMR Tests	13
3-2	A Comparison of Measured and Calculated Amplitude of Oscillation Due to Multipath for Rendezvous Radar WSMR Tests	15
3-3	Map of Rendezvous Radar WSMR Test Flights Exhibiting Off Boresight Tracking	17
A-1	Geometry for Calculating Period of Oscillation Due to Multipath	25
A-2	Effect of Reflecting Surface Cuvature on Multipath Geometry	29
B-1	Solution of Transcendental Equation for Amplitude of Oscillation Due to Multipath	32
C-1	Lunar Mission Multipath Geometry and Resulting Boresight Error	35
D-1	Received S/N Versus Range Between 0 n.mi. and 8 n.mi. in a 1 KHz Bandwidth	37
D-2	Received S/N Versus Range Between 0 n.mi. and 400 n.mi. in a 1 KHz Bandwidth	38

LIST OF SYMBOLS

AGC	Automatic Gain Control
B	Receiver Bandwidth in db
B.W.	Antenna Beamwidth
c	$\frac{(0.88)180°}{(3.3°)}$
D	Line-of-Sight Separation in feet
db	Decibel
$\vec{E}$	Electric Field Vector
ft	Feet
ft/sec	feet per second
g	Gravitational Acceleration at Earth's Surface
GAEC	Grumman Aircraft Engineering Corporation
G_{RR}	Gain of the Rendezvous Radar in db
G_T	Gain of the Transponder in db
h_r	Height of Receiver in feet
h_t	Height of Transmitter in feet
KTB	Receiver Input Noise in db
LGC	LM Guidance Computer
LM	Lunar Module
LOS	Line-of-Sight
MR	Milliradian
n.mi.	Nautical Mile
$\overline{NF}$	Noise Figure in db
P_t	Transmitted Power
R	Range in feet
RCA	Radio Corporation of America

LIST OF SYMBOLS (CONTINUED)

RF	Radio Frequency
RR	Rendezvous Radar
RR	Range Rate in ft/sec ($\dot{R}$)
RR/T	Rendezvous Radar/Transponder
S	Shaft Angle
(S/N)	Signal-to-Noise Ratio in db
sec	seconds of time
T	Transponder
V	Tangential velocity of transmitter in ft/sec
WSMR	White Sands Missile Range
α	Elevation Angle in Degrees
Δ	Change in a parameter
$\Delta\varepsilon_c$	Change in ε_c due to curvature of reflecting surface
ΔP	Change in pathlength in feet
δ	Phase shift of reflected signal with respect to direct signal
ε	Angle formed between line connecting transmitter and receiver, and tangent plane at transmitter
Θ	Amplitude of maximum boresight error in degrees
λ	Wavelength of transmitted signal in feet
π	3.1416
ρ	Ground reflection coefficient
Σ losses	Sum of the losses
σ	Standard Deviation
ψ	Grazing Angle in Degrees

1.0 INTRODUCTION

The results of the analysis of the Rendezvous Radar Test Flight Data from the White Sands Missile Range is presented in this report. A summary table is presented for quick reference. Correlation, as much as possible, was made with the White Sands Missile Range flight notes and RCA's "quick look analysis" in judging all data that was found out of specifications. This was particularly true in looking at range rate and range data where much of the data out of specification was caused by low transponder AGC and transponder "drop-out".

The overall performance of the Rendezvous Radar based on review of the White Sands Missile Range PEARL Flight Tests is very good. Most of the anomalies were caused by environmental phenomena such a multipath, antenna initial designation errors causing off boresight tracking, low transponder AGC and transponder "drop-out". A very small percentage of total data recorded contained anomalies which could possibly be attributed to the Rendezvous Radar.

The multipath phenomenon is covered in detail and the derivation of the period and amplitude of oscillation due to multipath is presented in the Appendix. Also presented in the Appendix is the application of the multipath phenomenon to the lunar mission, along with signal-to-noise versus range curves for additional reference.

2.0 GENERAL DISCUSSION OF RENDEZVOUS RADAR PEARL FLIGHT TESTS

The objective of the Rendezvous Radar (RR) PEARL Flight Tests was to evaluate the performance of the RR under flight conditions similar to those anticipated during the lunar mission. To realize this objective RR Antenna Assembly No. 7, RR Electronics Assembly No. 9, and Transponder No. 10 were tested at the White Sands Missile Range (WSMR).

2.1 PEARL CONFIGURATION

The flight test data were collected with the Rendezvous Radar mounted on a partial full-scale model of the LM. The model was located at the test site designated as PEARL at WSMR. The +Z LM Spacecraft Coordinate Axis was to the north and the LM model was pitched up +30° to facilitate simulation of overhead passes during lunar stay without actually tracking directly overhead.

2.2 FLIGHT PROFILES

The transponder was mounted aboard both a T-33 jet aircraft and an SH-3A helicopter. The flight paths shown in Figures 2-1 through 2-4 were flown to simulate different operating conditions.

North and south profiles exercised the shaft independent of the trunnion. East and west flights independently evaluated trunnion performance. Diagonal and circular patterns demonstrated the combined performances of shaft and trunnion.

The L- and H-profile tests were conducted in RR Mode II or lunar stay configuration.

The one B-profile test, RR-94B, was flown at close range using the SH-3A helicopter to simulate LM final rendezvous. RR-94B was run in Mode II also because the helicopter was hovering above the PEARL site. All other profiles were conducted in RR Mode I or rendezvous configuration.

Figures 2-1 through 2-4 contain maps of the various profiles flown.

Figure 2-1 shows the X, S, L, and H profiles.

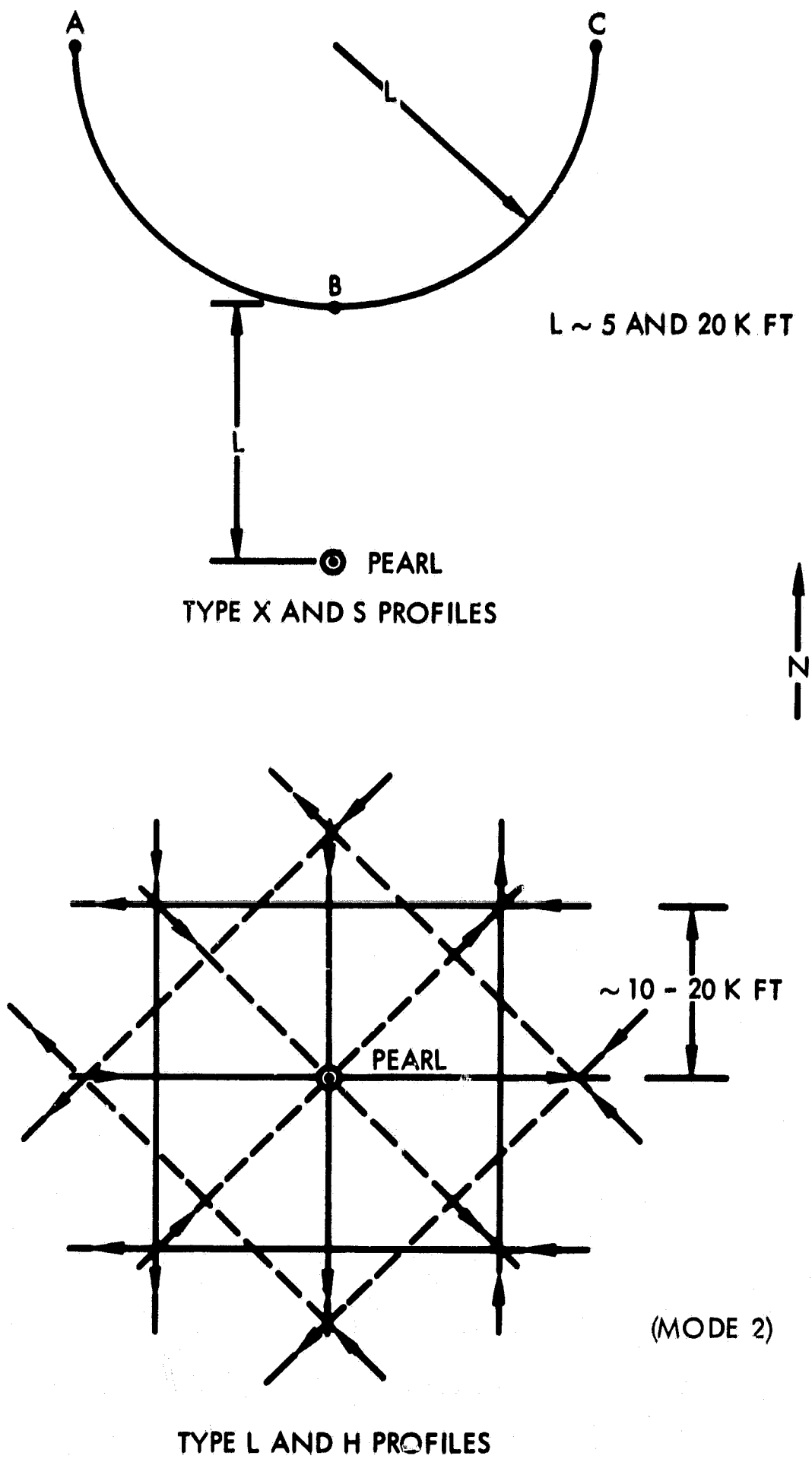

Figure 2-1. Maps of X,S,L and H Profiles Flown in Rendezvous Radar WSMR Tests

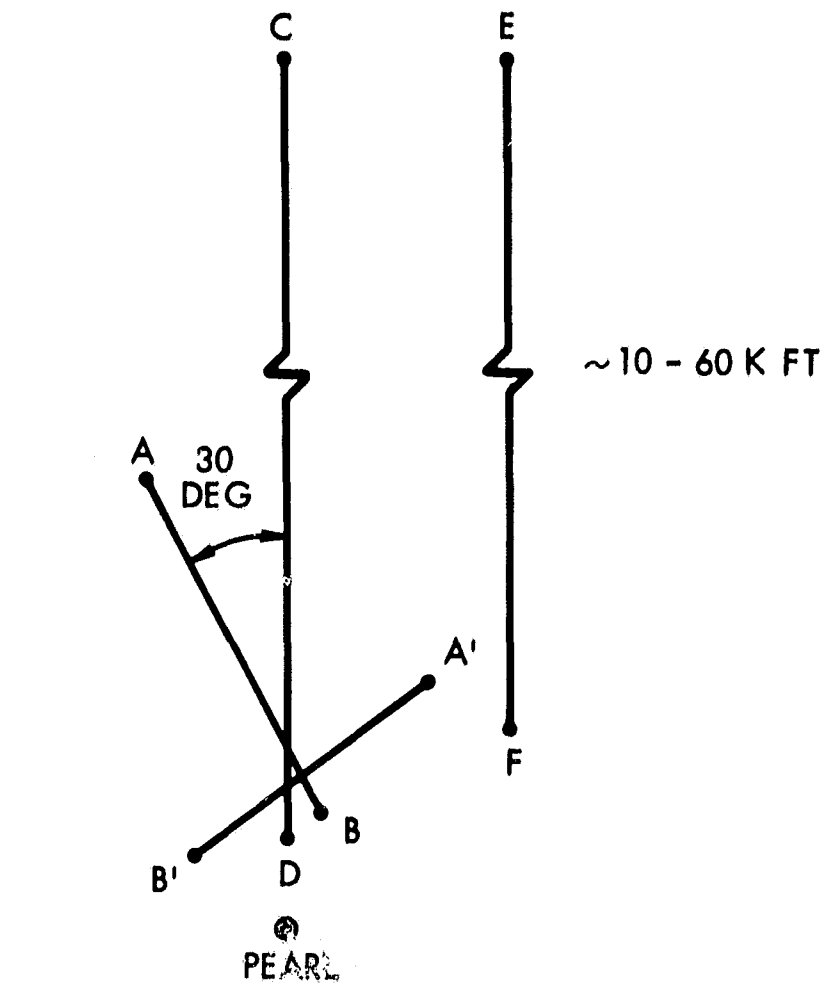

TYPE AA, W AND Z PROFILES

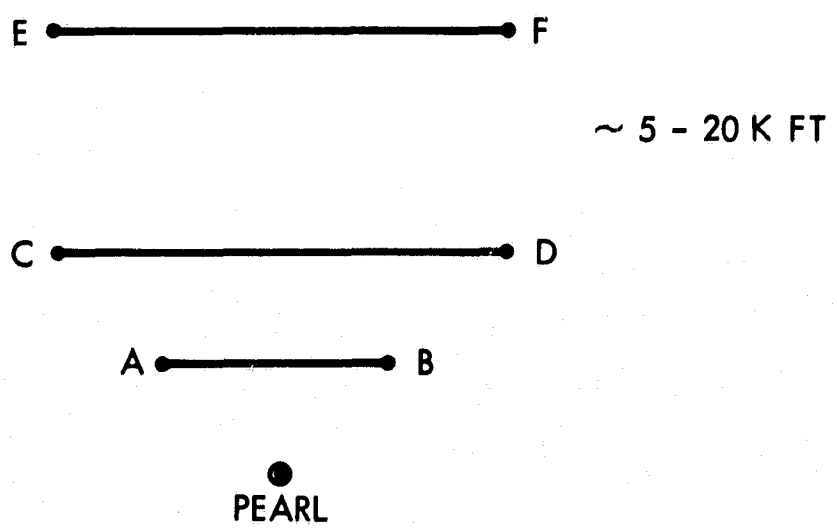

TYPE T AND Y PROFILES

Figure 2-2. Maps of AA,W,Z,T and Y Profiles Flown in Rendezvous Radar WSMR Tests

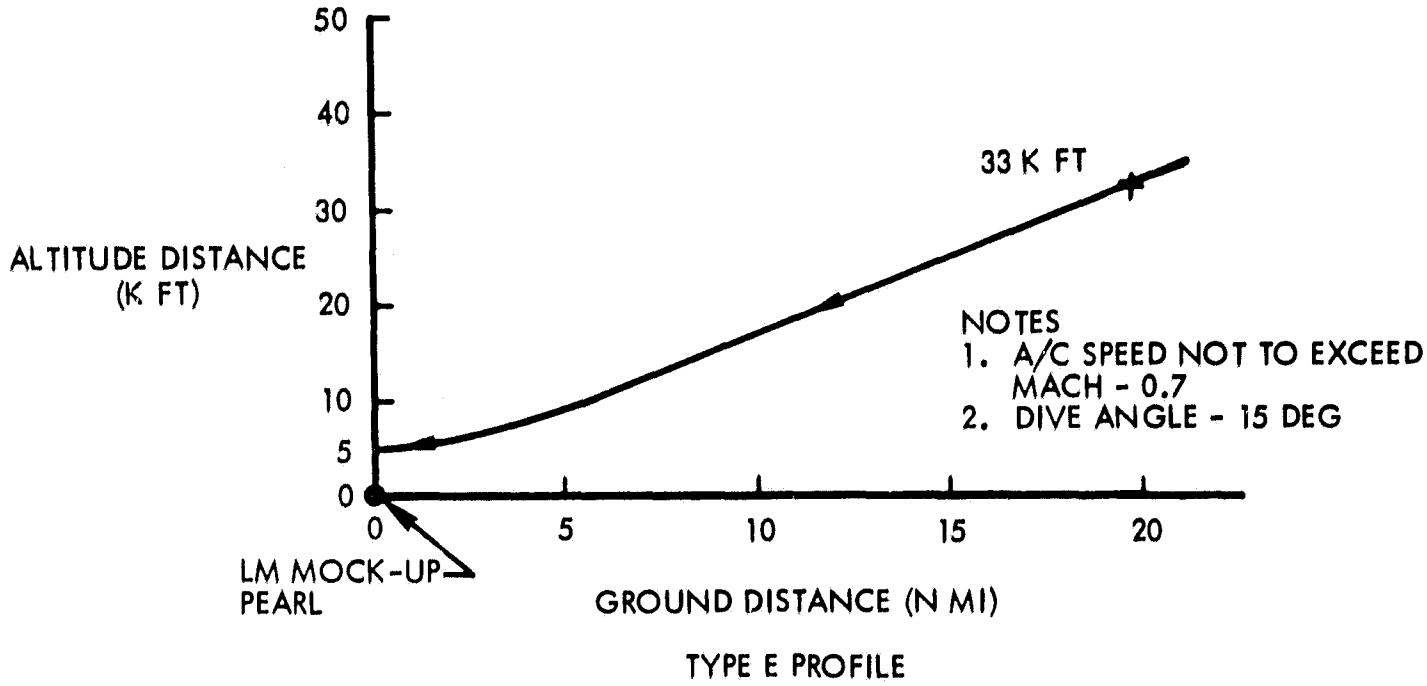

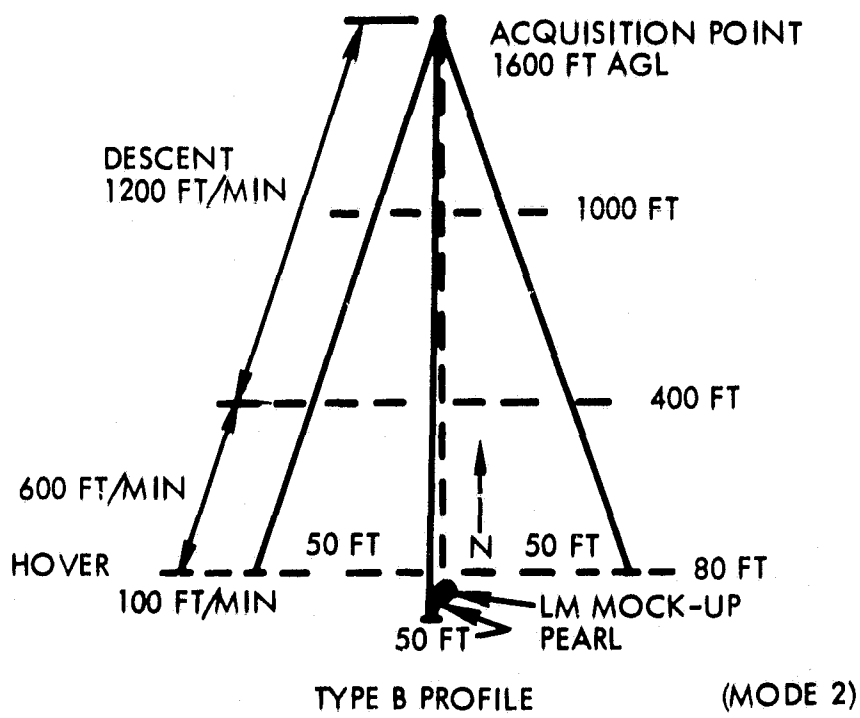

Figure 2-3. Maps of E and B Profiles Flown in Rendezvous Radar WSMR Tests

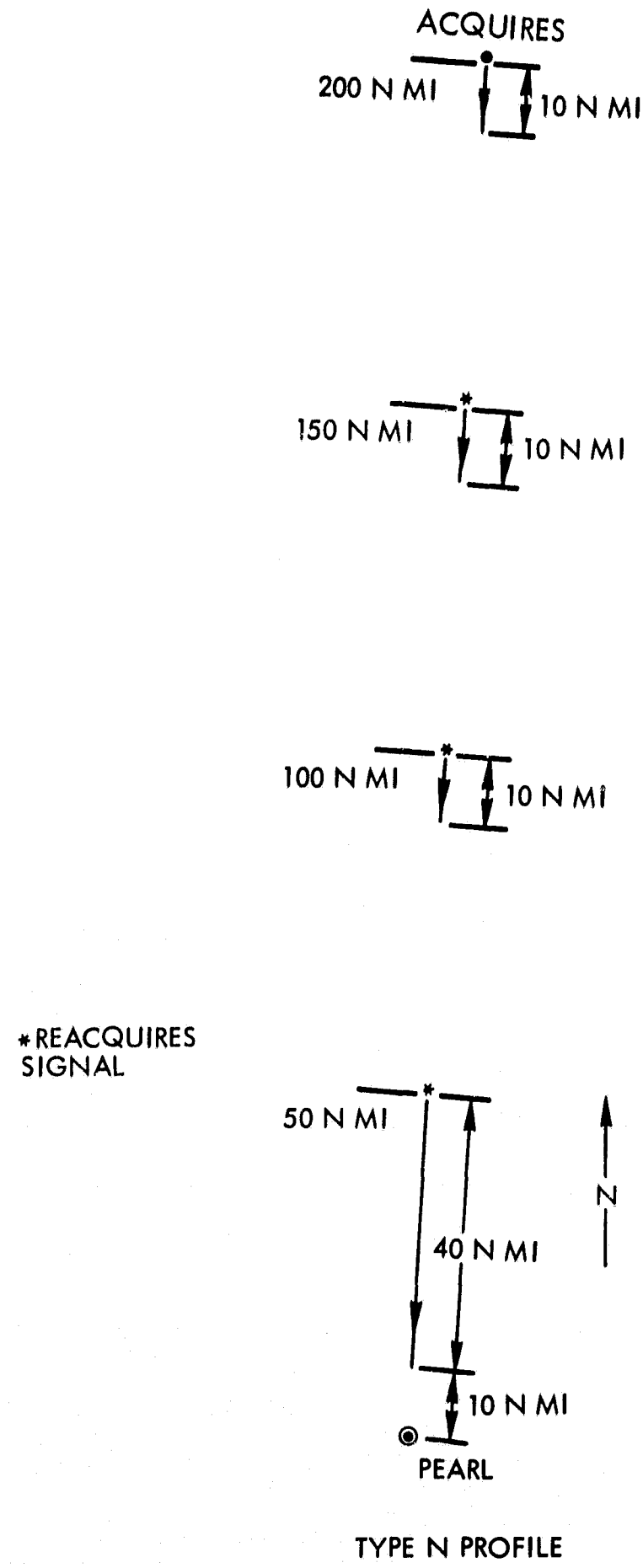

Figure 2-4. Map of N Profile Flown in Rendezvous Radar WSMR Tests

Figure 2-2 contains the AA, W, Z, T, and Y profiles.

Figure 2-3 gives the E and B profiles.

Figure 2-4 shows the N-profile, a long range profile used to evaluate the RR performance at maximum range and low elevation angles.

2.3 PARAMETERS MEASURED

The four parameters measured at WSMR during the RR PEARL tests were shaft angle, trunnion angle, range rate, and range. These parameters were measured by the RR and compared to similar measurements by either the WSMR Cinetheodolite optical measuring network or the WSMR AN/FPS-16 C-Band pulse radar. The error in the RR measurement of the four parameters was calculated by comparing the RR data to the reference Cinetheodolite or AN/FPS-16 data. After smoothing, these error values were plotted as a function of time for each flight and presented in WSMR National Range Data Reports.

2.4 DATA ANALYSIS PROCEDURE

Upon receipt of these reports, the error versus time curves were converted to error versus range curves by TRW for analysis purposes. For each flight the error curves for the parameters of shaft, trunnion, range rate and range error were compared with the Rendezvous Radar Specification (Table 2-1). Abnormal data (data out of specification) was reviewed and compared with White Sands Missile Range test flight notes [1] and RCA's "quick look analysis" [3] to isolate abnormal data that was subject to testing irregularities. Data exhibiting the multipath phenomenon was grouped together comparing period and amplitude of oscillation. In addition, data found not to be tracking on boresight was grouped together. Oddities in the measured parameters, such as range bit jitter, were investigated even though they were within specification.

Table 2-1. Rendezvous Radar Specifications

PARAMETER	RENDEZVOUS RADAR SPECIFICATION		
	CONDITION	RANDOM ERROR (3 SIGMA)	BIAS
Range Accuracy	RANGE > 50.6 NMI		±500 feet
	RANGE < 50.6 NMI		± 80 feet
	80 ft < RANGE < 5 NMI	1.0%/80 feet	
	5 NMI < RANGE < 400 NMI	0.25%/300 feet	
Range Rate Accuracy	ALL RANGES	1 fps	±1 fps
Angle Accuracy	ALL RANGES		±8 MR
	400 NMI	4 MR	
	300 NMI	3 MR	
	200 NMI	2 MR	
	5 NMI	2 MR	
	2 NMI	5 MR	
	1 NMI	10 MR	
	80 feet	10 MR	
Angle Rate Accuracy	400 NMI	0.4 MR/Sec	
	100 NMI	0.2 MR/Sec	

3.0 RESULTS OF RENDEZVOUS RADAR TEST ANALYSIS

The results of the Rendezvous Radar PEARL Flight Tests Analysis is presented in this section. The anomalies involving shaft, trunnion, range rate and range are reviewed in detail. The multipath phenomenon, off boresight tracking and the cause of low transponder AGC and transponder "drop-out" are presented.

3.1 SUMMARY OF RESULTS

Table 3-1 summarizes the results of the Rendezvous Radar Test Flight Series data analysis. The first column lists the flight number and profile along with the number of passes, in parenthesis, flown for that particular flight number and profile. In addition the flight tests of the same type of profile are grouped together. The maps of the profile types have been presented in Section 2.3.

The next four columns summarize the data that was found to be out of specification. A number found in these columns denotes that for that particular pass number of that flight number and profile, the parameter where the pass number is located is greater than the specified bias or three sigma value for the Rendezvous Radar.

The probable cause of the abnormal data is listed as a group in the next four columns. The "Multipath Effect" column lists, by rows, the abnormal data that exhibited the pronounced characteristics of the multipath phenomenon. It will be shown later how the multipath phenomenon was evaluated. The letters S and T found in this column refer to the shaft and trunnion respectively. These were previously designated in the shaft and trunnion columns of the Abnormal Data group. The notation of an S or T with the pass number, enclosed by parenthesis, denotes that pass was within specification but also exhibited multipath.

Table 3-1. Summary Table of Analysis of Rendezvous Radar PEARL Flight Test Data

RENDEZVOUS RADAR FLIGHT NUMBER - PROFILE (NUMBER OF PASSES)	ABNORMAL DATA (DATA EXCEEDING SPECIFICATION)				PROBABLE CAUSE OF ABNORMAL DATA				Range Simulator Used In Each Flight
	Shaft	Trunnion	Range Rate	Range	Multipath Effect	Off Boresight Tracking	Transponder Low AGC & Drop-Out	Comments	
92-AA (7)	2,4,7	1,2,4,7				S&T-2,4,7		T-1-Three Bad Points	80 N.M.
94-B (4)	1,2,3,4	1,2,3,4		1		S&T-1,2,3,4	R-1		None
66-E (2)	2	2	1,2				S&T-2	RR-1,2 Cause Unknown	None
85-E (5)			3,4,5					RR-3,4,5-Dive Profile	200 N.M.
88-E (10)	1,2,4,5,6		1-10					RR-1-10;Dive Profile S-1,2,4,5,6-Exceed Shaft Rate	200 N.M.
57-H (5)			1,3	2,3	(S-1)		R-2,3	RR-1,3-A/C Banking	80 N.M.
60-H (6)			1,2,3	1			RR-1,2,3;R-1		80 N.M.
74-H (2)			2					RR-2, Cause Unknown	80 N.M.
77-H (7)	1		1,4,5,7		S-1			RR-1,4,5,7;Cause Unknown	80 N.M.
82-H (6)	1,2,3,4,5,6	1,4,6	2,3,5	1,4,6		S&T-1,4,6	R-1,4,6,RR-3,5	S&RR 2,3,5-Mechanical Limit	80 N.M.
83-H (8)	1,3,5,7	1,3,5,7	2,3,4,5,6,7,8	1,3,5,7		S&T-1,3,5,7		R&RR-1,3,5,7-TPDR Shading RR-2,4,6,8-Cause Unknown	80 N.M.
75-L (4)			1,2				RR-1,2		80 N.M.
76-L (8)								ok	80 N.M.
54-N (3)	1,2,3		3		S-1,3	S-2		RR-3,Cause Unknown	200 N.M.
58-N (4)	1,2,3,4	1,3			S-1,2,4;T-1	S&T-3			None
61-N (6)								Bad Data-Radome Torn	None
65-N (4)	1,2,3,4	3	1		S-1,2,3,4;T-3			RR-1,Spike-Cause Unknown	None
68-N (4)	1,2,3,4	3	1		S-1,2,3,4;T-3			RR-1 Cause Unknown	None
73-N (4)	1,2,3,4		3		S-1,2,3,4			RR-3,Cause Unknown	200 N.M.
81-N (5)	2,3,4,5				S-2,3,4,5			S-2, 30-MR. Glitch Cause Unknown	200 N.M.
55-S (3)	1,3			1,2,3	S-1,3		R-1,2,3		80 N.M.
67-S (5)			1,2,3	1,2,3,5			RR-1,2,3;R-1,2 3,5		80 N.M.
72-S (8)			7	2,7			RR-7;R-2,7		80 N.M.
86-S (6)			1,2,3,5	5,6				R-5,6-Final 10 sec. RR-1,2,3,5 - Cause Unknown	80 N.M.
59-T (6)	5		3		S-5			RR-3 Cause Unknown	80 N.M.
71-T (5)					(S-1,2)			R-1,2-75 Ft Jitter	80 N.M.
84-T (6)			5,6	1,3,5	(S&T-1-6)		RR-5 R-1,3,5	RR-6-A/C Banking R-1,3,5-TPDR Shaded	80 N.M.
69-W (7)								R-5,7-Marginal	80 N.M.
70-W (4)			4					RR-4-Cause Unknown	80 N.M.
78-X (8)	5							S-5, Cause Unknown	80 N.M.
80-Y (7)	1,6,7	6,7	1		S-1	S&T-6,7	RR-1		80 N.M.
89-Y (9)	1,5,6	1,5,6,8				S&T-1,5		S&T-6-Bad Data T-8,Glitch-Cause Unknown	80 N.M.
93-Y (6)	1,6		1,2,3,6	1,3,6			R&RR-1,3,6	RR-2 Cause Unknown S-1,6 Cause Unknown	80 N.M.
90-Z (8)				2			R-2		80 N.M.

The column labeled "Off Boresight Tracking" summarizes all passes where the Rendezvous Radar was tracking off boresight. This will be discussed further in the next section. The column labeled "Transponder Low AGC and Drop-Outs" shows the abnormal data that is believed to be caused by the transponder having a low AGC or dropping out of lock. The letters RR and R found in this column denote Range Rate and Range respectively with their corresponding pass numbers. Again, the passes noted here were previously noted in the "Abnormal Data" group of this table.

The column labeled "Comments" lists the remainder of the abnormal data not falling into the classification of the preceeding three columns. This column will also be expounded upon in greater detail in the next two sections of this report. The last column of Table 3-1 specifies the amount of added range simulation used for each flight test series. In order to simulate longer ranges, an attenuator was placed in the R.F. line between the Transponder Antenna Assembly and the Electronics Assembly, and a phase shifter (Special Range Simulator) was inserted at the Rendezvous Radar to shift the phase of the incoming signal.

3.2 SHAFT AND TRUNNION

The shaft and trunnion data found to be out of specification and noted in Table 3-1 were analyzed and the probable causes listed in the Table. In order to evaluate data where multipath is suspected it was necessary to calculate the period and amplitude of the oscillation of the Rendezvous Radar Antenna. This oscillation in the antenna tracking occurs because the antenna tracks a composite phase front formed by the combination of a direct signal (direct path from Transponder to Rendezvous Radar) and a reflected signal (indirect path from Transponder to Rendezvous Radar by reflection from the ground). As the Transponder position changes, the phase relationship between the direct and indirect signal changes and the phase front characteristics change. In the case of the Rendezvous Radar PEARL flight tests, the change of the Transponder position was nearly uniform in the direction of flight, thus causing the phase front to vary in a cyclic fashion. This causes the Rendezvous Radar to track in an oscillating motion which is evidenced in recorded data of certain flights. The derivations and geometry involved in predicting the multipath phenomenon are presented in the Appendix.

The period of oscillation due to multipath can be calculated by

$$\Delta t = \frac{D^2}{\left(\frac{2h_r}{\lambda}\right)(h_t + \Delta\varepsilon_c D)\, v} .$$

Figure 3-1 shows examples of multipath taken from the recorded data. Table 3-2 shows a comparison between measured periods of oscillation and calculated periods of oscillation due to multipath for several flights and profiles. This table shows the close agreement between measured and calculated periods of oscillation.

The amplitude of shaft oscillation due to multipath can be determined from curve (c) shown in Figure 3-2. This curve applies primarily to the region where the elevation angle (α) is equal to or greater than the beamwidth of the receiving antenna ($\geq 3.3°$ for Rendezvous Radar). Curve (c) fits very closely the Rendezvous Radar data for angles less than the beamwidth. An exact expression for the maximum boresight error due to multipath for all angles is presented in the Appendix. Figure 3-2 also shows the amount of bias introduced by the multipath phenomenon. A further comparison of measured and calculated amplitude of oscillation due to multipath is shown in Table 3-3.

The passes noted in the "Multipath Effect" column of Table 3-1 were judged to be out of specification due to the multipath phenomenon after comparing their oscillatory nature with the two above criteria of period and amplitude.

The passes noted under "Off Boresight Tracking" in Table 3-1, with the exception of pass 2 of flight 94-B, are mapped on Figure 3-3, and represent cases where tracking in side lobe regions occurred. Pass 2 of flight 94-B was initially tracking off boresight, but was redesignated to on boresight tracking for the remainder of the flight. The map boundaries and lock-points were obtained from September's Radar Integration Meeting Notes [4]. This information was supplied by Grumman Aircraft Engineering Corporation. The original map also indicated the four outer lock points

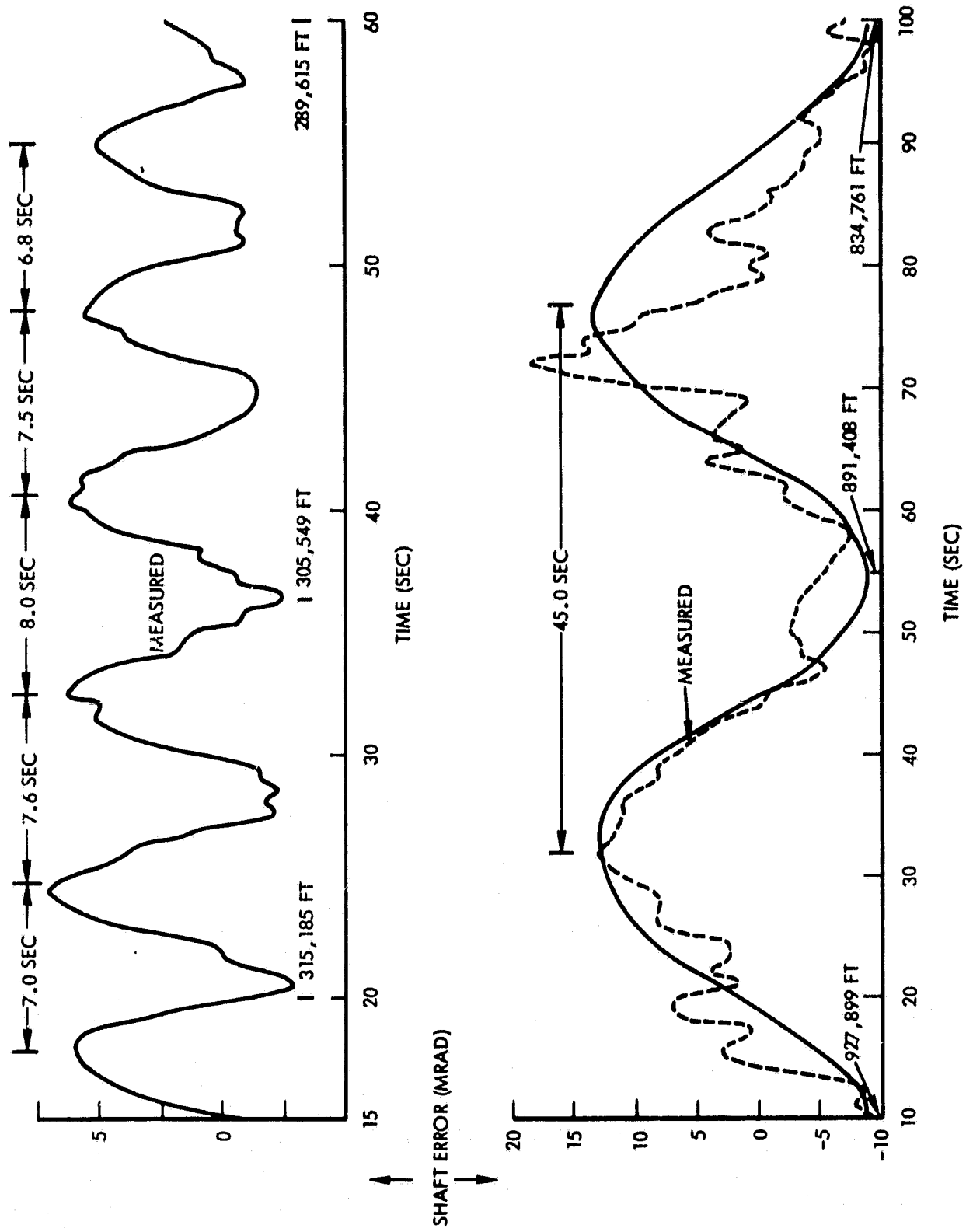

Figure 3-1. Examples of Multipath Taken From Recorded Data of the Rendezvous Radar WSMR Tests

Table 3-2. Comparison of Measured and Calculated Period of Oscillation Due to Multipath for Rendezvous Radar PEARL Test Flights

Flight Number RR-	Range (Ft.)	Measured Period of Oscillations (SEC)	Calculated Period of Oscillations (SEC)
54N, Pass 1	830,000	58	58.0
81N, Pass 3	891,000	45	44.5
81N, Pass 4	547,000	22	21.5
54N, Pass 3	290,000	11	11.3
81N, Pass 5	305,500	7.5	7.55
59T, Pass 5	44,200	3.8	3.7

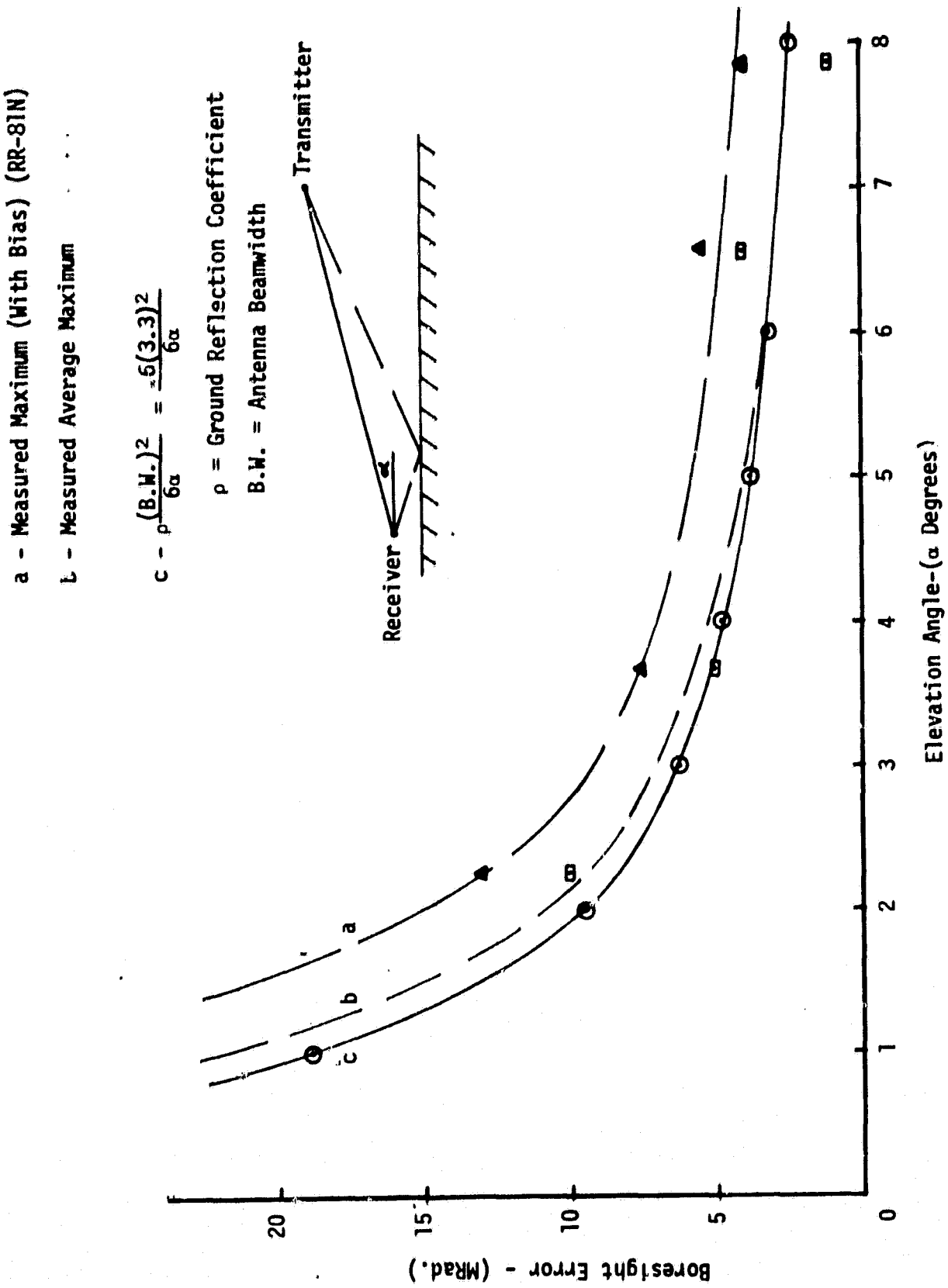

Figure 3-2. A Comparison of Measured and Calculated Amplitude of Oscillation Due to Multipath for Rendezvous Radar WSMR Tests

Table 3-3. Comparison of Measured and Calculated Amplitude of Oscillation Due to Multipath for Rendezvous Radar PEARL Test Flights (Boresight Error)

Flight Number RR-	Range (Ft.)	Measured Amplitude of Shaft Oscillations (MR)	Calculated Amplitude of Shaft Oscillation (MR) $(\rho\frac{(B.W.)^2}{6\sigma}, \rho=.6)$
54N, Pass 1	830,000	±11	±9
81N, Pass 3	891,000	±10	±8.5
81N, Pass 4	547,000	± 5	±5.2
54N, Pass 3	290,000	± 4.8	±3.2
81N, Pass 5	305,500	± 4	±3.0
59T, Pass 5	44,200	± 1.4	±1.2

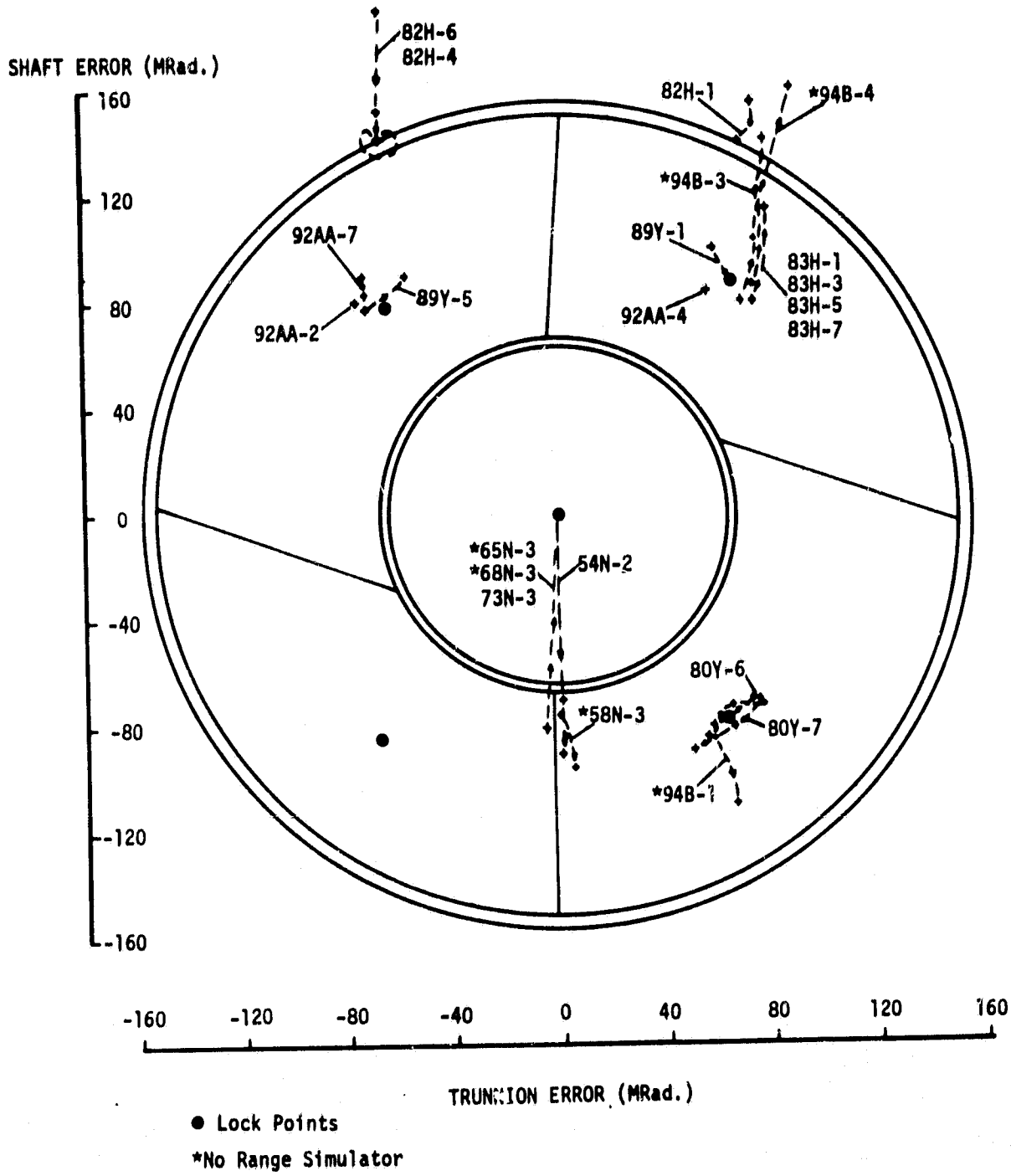

Figure 3-3. Map of Rendezvous Radar WSMR Test Flights Exhibiting Off Boresight Tracking

were stable lock points if the path loss was less than 87 db or the separation between Rendezvous Radar and Transponder was less than 30 nautical miles. In addition, the Rendezvous Radar would slew into the lock point represented in each of the five zones shown from any point in the zone when auto track was enabled. The asterisk above the flight number-profile-pass indicates those flights where no range simulator was used. All other flights mapped would have at least an eighty nautical mile range simulator and according to the above mentioned criteria would not experience stable side lobe locks at the outer lock positions indicated in Figure 3.3. Flights 65N-3 and 68N-3 are long profile flights and their separation is also much greater than 30 nautical miles. Therefore, the only flights that should experience side lobe lock-up based on the 30 nautical mile criterion are 94B-1, 94B-3, and 94B-4. In each of these cases the Rendezvous Radar Antenna was driven away, not into, the nearest lock point. For this particular flight profile, the attitude of the helicopter was changing significantly and may have aggravated the tracking.

The profiles that appear to be at a fairly stable lock in the vicinity of a side lobe lock point are outside the 30 nautical mile minimum range. This may imply that the received signal strength is higher than would normally be expected at their respective ranges. This could possibly be caused by such things as greater than 0 db gain in the transponder antenna and other optimum performing components throughout the system, raising the actual signal-to-noise ratio. As is generally recognized, side lobe lock-up is a definite possibility, but may occur at ranges greater than the 30 natuical miles mentioned earlier.

Additional discussion of shaft (S) and trunnion (T) data noted in the "Comments" section of Table 3.1 will now be presented. The trunnion data of flight 92-AA pass 1 was only out of specification at three points of a total 120 points and may have been caused by transponder "drop-out". The cause of transponder dropping out of phase lock will be covered in Section 3.3 The shaft data of flight 88-E passes 1, 2, 4, 5, and 6 were out of specification at the end of the flight. This occurs when the aircraft initiates a six "g" pull-up from the dive profile that ends in

straight and level flight. For this case the shaft rate may have been exceeded. In flight 82-H passes 2, 3, and 5 the Rendezvous Radar Antenna went into mechanical limit of the shaft and experienced transponder "drop-outs". The cause of the 30 MR glitch in shaft data of flight 81-N pass 2 had no apparent explanation in the flight notes. The remainder of the flight was within specification. The 30 MR glitch may have been caused by interference from the reflected signal which experienced diffraction from a terrain irregularity. The shaft data of flight 78-X pass 5 experienced a ten second disturbance in the center of the flight of ± 4 MR peak-to-peak. No apparent cause for this disturbance was found in the flight notes, but due to the small magnitude and short duration and occurrence in only one out of eight passes it is not of major concern. The shaft and trunnion data of pass 6 of flight 89-Y were considered as bad data and were not used in judging the performance of the Rendezvous Radar. Finally, the shaft data of passes 1 and 6 of flight 93-Y are out of specification during the first part of each flight. The exact cause is not known but similar T profile flights experienced pronounced multipath at the beginning and end of their passes.

3.3 RANGE RATE

The RR measures the two-way doppler shift of the signal received at the RR compared with the signal transmitted by the RR. The maximum theoretical error caused by losing or gaining a cycle in the 0.1 sec doppler sampling time is ± 0.5 ft/sec which is less than the specified 1 ft/sec 3σ error.

Range rate is measured in the Cinetheodolite System by a Δ range/Δ time computation. Typical Cinetheodolite 3σ range errors are less than 1.5 ft/sec. However, larger Cinetheodolite errors did occur in some instances such as the 2.16 ft/sec 3σ range rate error at 73230.399 seconds into flight RR-95AA. Hence, the predicted accuracy of the system to be measured often exceeds the accuracy of the standard of measure, and range rate performance analysis under these conditions is speculative. However, with this consideration in mind, an analysis was made of the range rate data combining both the specified RR 3σ error and Cinetheodolite error.

The 3σ range rate error of the AN/FPS-16 radar is greater than or equal to that of the Cinetheodolite. Hence, analysis of range rate data compared with this standard was also performed under the conditions stated in the previous paragraph.

Only when the range rate 3σ error was obviously out of the combined specification (4-5 ft/sec) was it noted as abnormal in Table 3-1. Of the 192 total passes of all flights 60 contained 3σ range rate errors which were out of specification or 31.2%. Of the 60 out of specification 15 were caused by a 17.6 db drop in the transponder AGC and a corresponding drop lock in the transponder tracking loop. GAEC/WSMR has stated that these transponder failures were caused by a loose cap on the diode mixers in the RF section of the transponder. Upon diagnosis and repair by RCA, normal transponder operation occurred.

During flights RR-83H, passes 1, 3, 5, and 7 and RR-84T passes 1, 3, and 5 the fuselage of the aircraft shaded the transponder from the Rendezvous Radar causing low signal level and large 3σ range rate error.

During passes 2, 3, and 5 of flight RR-82H, the RR antenna went into the mechanical limits of rotation and the range rate data became bad at that time.

In all the E-profile flights (RR-66E, RR-85E, and RR-88E) the range rate data was particularly poor. In this profile the T-33 jet aircraft is making a shallow dive 2 n.mi. north of PEARL at a speed of 300 knots and pulls up in a six "g" climb 0.5 n.mi. from PEARL. With this high velocity (506 ft/sec) at short ranges any attitude variations in the aircraft could produce significant changes in the Δ range measurement for computing the Δ range/Δ time Cinetheodolite range rate measurement. Also the attitude of the aircraft itself is changing rapidly, especially during the banking maneuver. Therefore, although the speed of the aircraft might be reasonably constant, the velocity of the transponder might vary significantly, causing the RR range rate measurement to differ from that of the Cinetheodolite. The comments in Table 3-1 regarding the remaining range rate

data which exceeds specification state "cause unknown" or "aircraft banking". A positive reason for this abnormal operation has not been proved but a possible answer is as follows. These anomalies occurred at the beginning and end of a flight when the aircraft was probably banking. Hence, the attitude of the aircraft was again changing rapidly and changes which the doppler measuring system could detect might not be sensed by the Cinetheodolite Δ range/Δ time measurement.

In general, the performance of the RR range rate measurement was very good. Anomalies were generally caused by transponder drop-outs and perhaps limitations in the Cinetheodolite range rate measurements.

The range rate bias error was consistently within the specified ± 1 ft/sec.

3.4 RANGE

Range is measured in the Rendezvous Radar by comparing the phase of the transmitted and received ranging tones. The magnitude of the range is digitized in the 18 bit Up-Down Range Counter. At ranges less than 50.6 n.mi. the 15 least significant bits in the Up-Down Range Counter are used in the 15 bit parallel shift to the LGC via the Signal Data Processor. The least significant bit in this case is 9.375 ft. If the range is greater than 50.6 n.mi. the 15 most significant bits in the Up-Down Range Counter are used with the least significant bit being 75 ft.

To simulate ranges similar to those to be encountered in a lunar mission, devices were placed in the range tracking loop to simulate both the attenuation and phase delay of longer ranges. The RF loss was simulated by placing attenuation in the transponder RF line between the Transponder Antenna Assembly and the Transponder Electronics Assembly. To simulate phase, the Special Range Simulator (SRS) was placed in the Rendezvous Radar between the Antenna Assembly and the Electronics Assembly. This SRS delayed the ranging tones in time comparable to 80 or 200 nautical miles. The flights which used this simulator are noted in the last column of Table 3-1.

The amplitude and phase range simulation devices were always matched to give a consistent addition of range in both amplitude and phase.

The specified limits on range bias and 3σ error are contained in Table 2-1. On flights which contained the range simulators, the allowable limits on range errors had to be extended accordingly. Flights in which the actual range was less than 50.6 n.mi. but which contained either the 80 n.mi. or the 200 n.mi. range simulator had the bias specification on range increased from ±80 ft to ±500 ft. When used, the 80 n.mi. of range simulation added 1216 ft to the existing 3σ error at a particular range. Similarly the 200 n.mi. of range simulation, when used, gave 3040 ft of additional 3σ error allowance.

With this added error margin only 29 of the 192 passes flown were out of the 3σ range specification. Of the 29 passes, 23 had range errors due to loss of lock by the Transponder. This was caused by a loose cap on the diode mixers in the RF section of the Transponder as explained in Section 3.3.

Of the remaining 6 passes, 4 were caused by the aircraft fuselage shading the Transponder during passes 1, 3, 5, and 7 of flight RR-83H.

The last two out of specification passes were passes 5 and 6 of flight RR-86S. The data was out of the 3σ error specification only during the last 10 seconds of each pass.

The range bias error was within the specified values for all passes.

In flight RR-71T the range data was within specification but an interesting phenomenon was noted. The range error was varying in a saw-tooth manner with an amplitude of 75 ft. This phenomenon was caused by the digitizing of the range in the 18 bit Up-Down Counter. With the 80 n.mi. of simulation, the least significant bit was 75 ft and hence the error would increase until the 75 ft bit changed state and drove the error back to the bias level.

With 20 total seconds of range data exceeding specifications due to problems other than transponder anomalies, compared to the more than 20,000 seconds of range data in the 192 passes, the performance of the RR ranging system, on the basis of these PEARL tests, is outstanding.

4.0 CONCLUSIONS

The performance of the Rendezvous Radar, judged by the PEARL Flight Test Series, is very good.

Very few anomalies could possibly be assigned to the Rendezvous Radar. Most of the data which exceeded specified error limits did so because of multipath, transponder problems, or other phenomena external to the Rendezvous Radar.

Since the multipath phenomenon could very well increase shaft and trunnion angular error beyond specified limits during the lunar mission, as shown in Appendix C, an analysis should be made of the effect of this phenomenon on the lunar surface.

APPENDIX A

DERIVATION OF THE PERIOD OF SHAFT OSCILLATION DUE TO MULTIPATH

When electromagnetic waves are propagated above a reflecting surface, and both the transmitter and receiver are above, yet relatively close, to the reflecting surface, the wave incident upon the receiver is the composite $\vec{E}$ field consisting of the direct and reflected $\vec{E}$ fields added vectorally. For a linearly polarized $\vec{E}$ field transmitted above a perfectly reflecting, smooth but not necessarily flat surface, at grazing angles (ε) below the Brewster angle (about 20° for the earth at X-band), the phase front of the composite $\vec{E}$ field will be linear and will vary sinusoidally with time if the relative velocity between the transmitter and receiver is constant and non-zero and if the displacement of the transmitter and receiver above the reflecting surface is constant and non-zero. The phase of the composite signal will be a function of the path length difference between the direct and reflected paths.

Consider Figure A-1. The period of oscillation will first be derived for a flat reflecting surface and then modified to satisfy a spherical reflecting surface.

A macroscopic view of both transmitter and receiver is shown. Because of the great difference in transmitter height, h_t (on the order of 10^4 feet), and receiver height, h_r (on the order of 10^1 feet), and because of the large line-of-sight (LOS) separation between the transmitter and receiver, D (on the order of 10^4 to 10^5 feet), the receiver appears to be on the reflecting surface. However if the receiver microscopic view is considered, the direct and reflected rays can be seen.

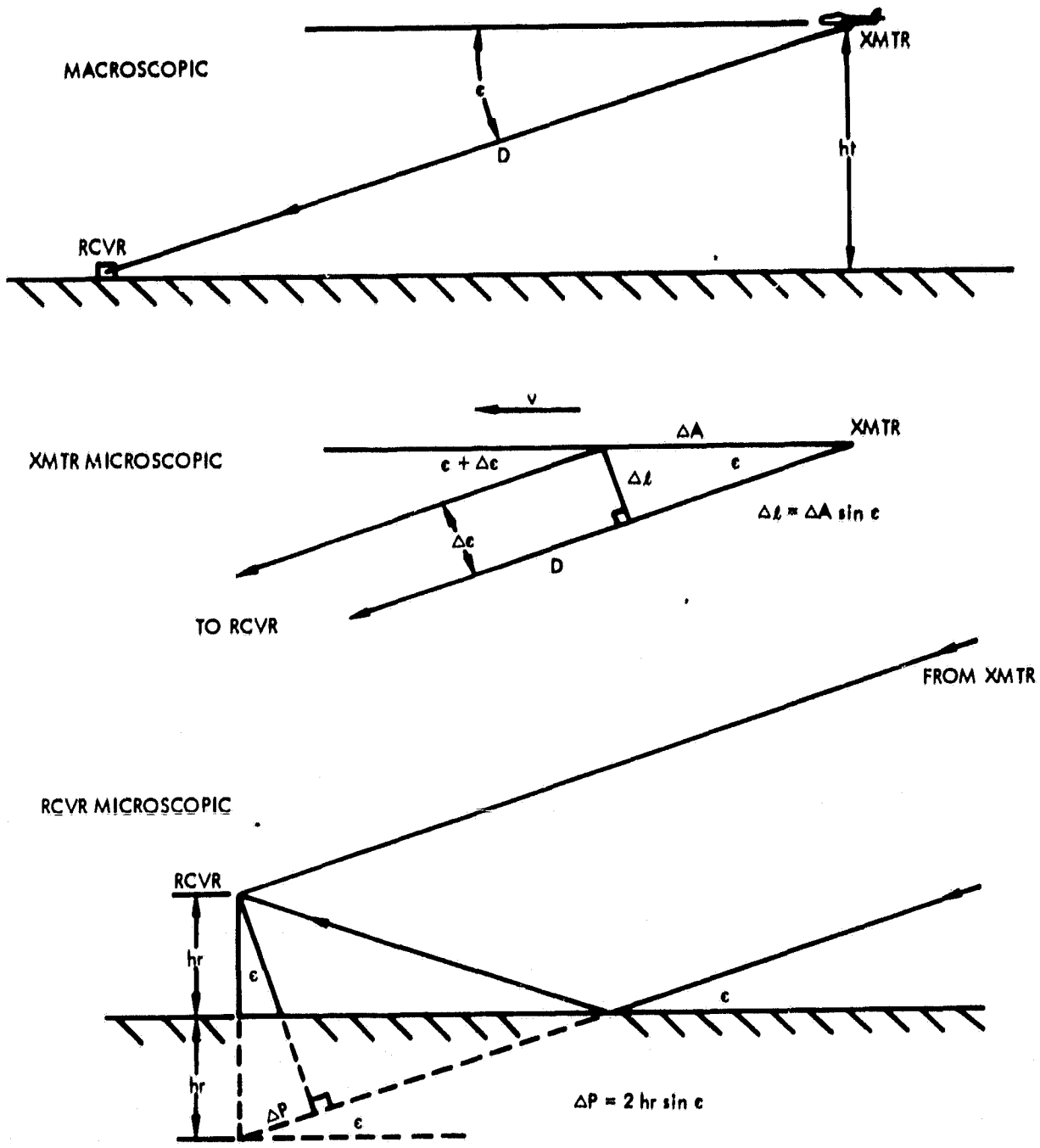

Figure A-1. Geometry for Calculating Period of Oscillation Due to Multipath

Consider the difference in the direct and reflected path lengths ΔP

$$\Delta P = \left(\frac{2h_r}{\lambda}\right) \lambda \sin \varepsilon \qquad \text{(A-1)}$$

where

ΔP = difference in path length in feet

h_r = height of receiver above the reflecting surface in feet

λ = wavelength of signal in feet

ε = grazing angle in radians

Divide (A-1) by Δt and take limit as $\Delta t \to 0$

$$\lim_{\Delta t \to 0} \frac{\Delta P}{\Delta t} = \frac{dP}{dt} = \left(\frac{2h_r}{\lambda}\right) \lambda \cos \varepsilon \frac{d\varepsilon}{dt} \quad . \qquad \text{(A-2)}$$

In the $\lim_{t \to 0} \frac{\Delta P}{\Delta t} = \frac{dP}{dt}$ hence,

$$\frac{\Delta P}{\Delta t} = \left(\frac{2h_r}{\lambda}\right) \lambda \cos \varepsilon \frac{\Delta \varepsilon}{\Delta t} \quad . \qquad \text{(A-3)}$$

Now consider the transmitter microscopic view

$$\Delta \varepsilon = \frac{\Delta \ell}{D - \Delta A \cos \varepsilon}$$

$$\Delta A << D \quad .$$

Therefore,

$$\Delta \varepsilon \approx \Delta \ell / D \qquad \text{(A-4)}$$

But

$$\Delta \ell = \Delta A \sin \varepsilon$$

and hence (A-4) becomes

$$\Delta \varepsilon \approx \frac{\Delta A \sin \varepsilon}{D} . \tag{A-5}$$

Substituting (A-5) into (A-3),

$$\frac{\Delta P}{\Delta t} = \left(\frac{2h_r}{\lambda}\right) \lambda \, (\cos \varepsilon) \, \frac{\sin \varepsilon}{D} \frac{\Delta A}{\Delta t} . \tag{A-6}$$

Since ε is small $\cos \varepsilon \rightarrow 1$. Macroscopically it can be seen that $\sin \varepsilon \approx h_t/D$. $\frac{\Delta A}{\Delta t}$ is the velocity of the transmitter (v) since it was stipulated that the transmitter is to be at constant height and velocity. Hence (A-6) becomes

$$\frac{\Delta P}{\Delta t} = \left(\frac{2h_r}{\lambda}\right) \lambda \frac{h_t}{D^2} v$$

and solving for ΔP,

$$\Delta P = \left(\frac{2h_r}{\lambda}\right) \lambda \frac{h_t}{D^2} v \, \Delta t \quad . \tag{A-7}$$

To find the period let the path length difference ΔP equal λ and solve for Δt, the period of oscillation:

$$\Delta t = \frac{D^2}{\left(\frac{2h_r}{\lambda}\right) h_t \, v} \tag{A-8}$$

The above solution is for the flat reflector case. Curvature of the reflecting surface will affect the angle $\Delta\varepsilon$ and the correction angle due to curvature is $\Delta\varepsilon_c$. $\Delta\varepsilon_c$ is not simply the angle between the tangent planes of the transmitter and receiver since there is another effect. Since the velocity of the aircraft is tangent to the reflecting surface at the transmitter, the transmitter will appear to rise to an observer at the receiver for a closing velocity. This effect tends to decrease $\Delta\varepsilon_c$ and the changing angle between the planes tends to increase $\Delta\varepsilon_c$. The latter is the dominant factor and a value of one half the angle between the tangent planes accounts for both factors. This angle is shown in Figure A-2.

The correction term $\Delta\varepsilon_c$ must be added to (A-6) giving

$$\frac{\Delta P}{\Delta t} = \left(\frac{2h_r}{\lambda}\right)\lambda \frac{\cos\varepsilon \sin(\varepsilon + \Delta\varepsilon_c)\, v}{D} \tag{A-9}$$

$$\sin(\varepsilon + \Delta\varepsilon_c) = \sin\varepsilon \cos\Delta\varepsilon_c + \cos\varepsilon \sin\Delta\varepsilon_c$$

$$\cos\Delta\varepsilon_c \approx \cos\varepsilon \approx 1 .$$

Therefore

$$\sin(\varepsilon + \Delta\varepsilon_c) \approx \sin\varepsilon + \sin\Delta\varepsilon_c \quad .$$

Hence (A-9) becomes

$$\frac{\Delta P}{\Delta t} = \left(\frac{2h_r}{\lambda}\right) \lambda \frac{v}{D} \left[\sin\varepsilon + \sin\Delta\varepsilon_c\right] .$$

Since $\sin\varepsilon = \frac{h_t}{D}$ and dividing by D

$$\frac{\Delta P}{\Delta t} = \left(\frac{2h_r}{\lambda}\right) \lambda \frac{v}{D^2} (h_t + \Delta\varepsilon_c D) \tag{A-10}$$

let $\Delta P = \lambda$ and solve for Δt

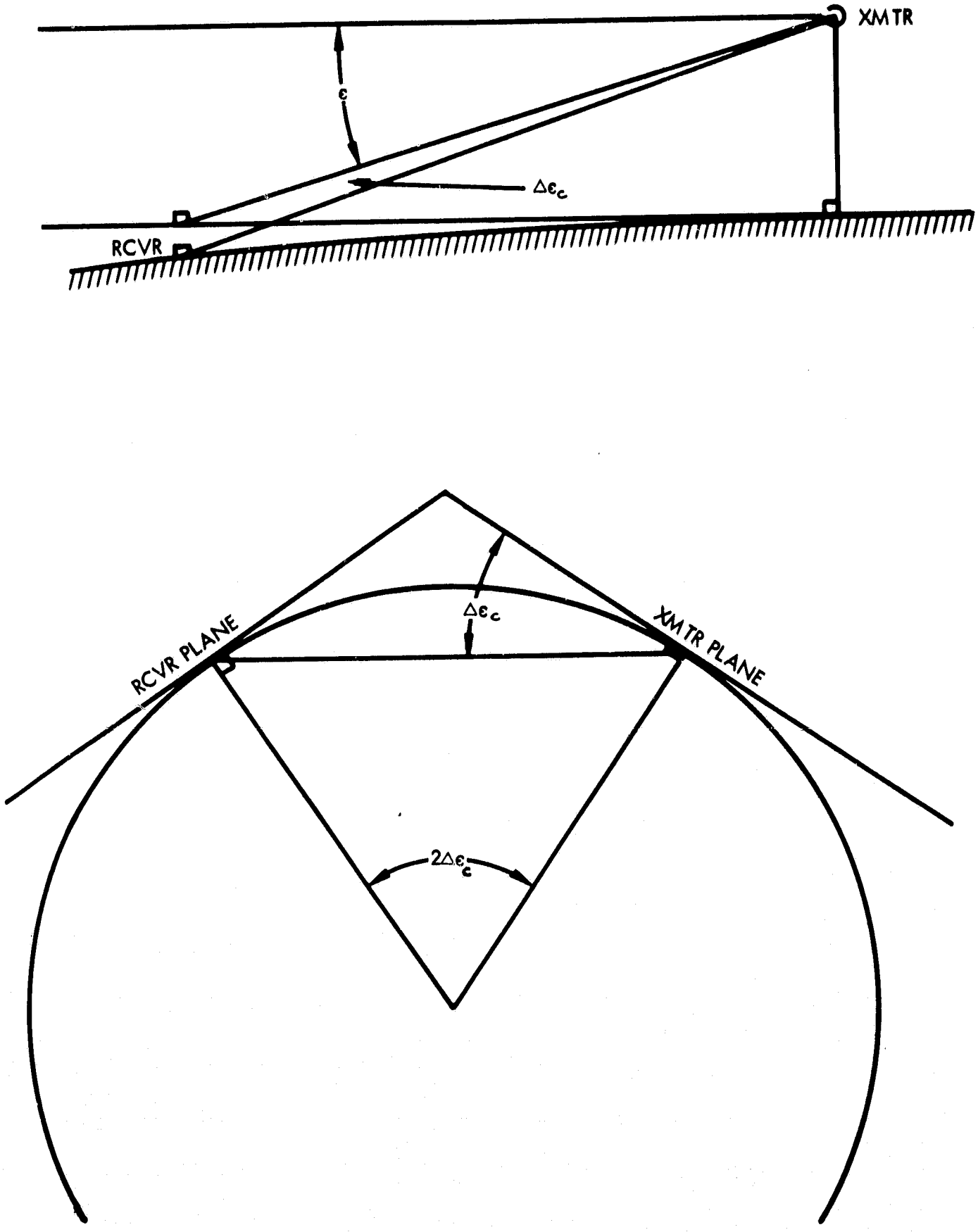

Figure A-2. Effect of Reflecting Surface Cuvature on Multipath Geometry

$$\Delta t = \frac{D^2}{\left(\frac{2h_r}{\lambda}\right)(h_t + \Delta\varepsilon_c D)\, v} \qquad \text{(A-11)}$$

where

Δt = period of oscillation in seconds

D = LOS separation between transmitter and receiver in feet

h_r = height of the receiver above the reflecting surface in feet

h_t = height of the transmitter above the reflecting surface in feet

λ = wavelength of the transmitted signal in feet

v = tangential velocity of the transmitter in feet per second

$\Delta\varepsilon_c$ = Correction in the angle between the line connecting transmitter and receiver, and the tangent plane to the reflecting surface at the transmitter, due to curvature of the reflecting surface, in radians. Approximately equals half the angle formed between the tangent planes at transmitter and receiver

(A-11) describes the period of shaft oscillation due to multipath in terms of parameters either readily available or easily calculated.

APPENDIX B

DERIVATION OF THE AMPLITUDE OF SHAFT OSCILLATION DUE TO MULTIPATH

The amplitude of oscillation due to multipath can be determined by solving the following transcendental equation:

$$\frac{\sin[c\,\sin(\Theta + 1.65°)]}{\sin(\Theta + 1.65°)} - \frac{\sin[c\,\sin(\Theta - 1.65°)]}{\sin(\Theta - 1.65°)}$$

$$+ \left\{\frac{\sin[c\,\sin(\Theta + 2\alpha + 1.65°)]}{\sin(\Theta + 2\alpha + 1.65°)} - \frac{\sin[c\,\sin(\Theta + 2\alpha - 1.65°)]}{\sin(\Theta + 2\alpha - 1.65°)}\right\} \rho \cdot e^{j\delta} = 0 \; .$$

where

$c = \frac{.88\pi}{B.W.}$

Θ = maximum amplitude (boresight error) in degrees

α = elevation angle in degrees

ρ = ground reflection coefficient

δ = phase difference between direct and reflected signals

The solution of this equation was performed and yielded the two solid curves in Figure B-1. The phase term $e^{j\delta}$ was set to $\pm 1 (\delta = 0, \pi)$ which represents the two extreme cases where the direct and reflected signals add in phase or out of phase. The multipath geometry was presented in Appendix A and is also indicated in Figure B-1. The first two terms of the above equation represent the difference pattern for the direct signal entering an amplitude monopulse antenna system. The third term represents the difference pattern for the reflected signal entering the same amplitude monopulse antenna system. The condition for stable lock along the boresight axis of an amplitude monopulse antenna system is that the sum of these two difference patterns be equal to zero or the error signal in servo loop be driven to zero. With the phase term having been set to ± 1 and ρ being specified, the envelope of the maximum boresight error can be determined from the transcendental equation.

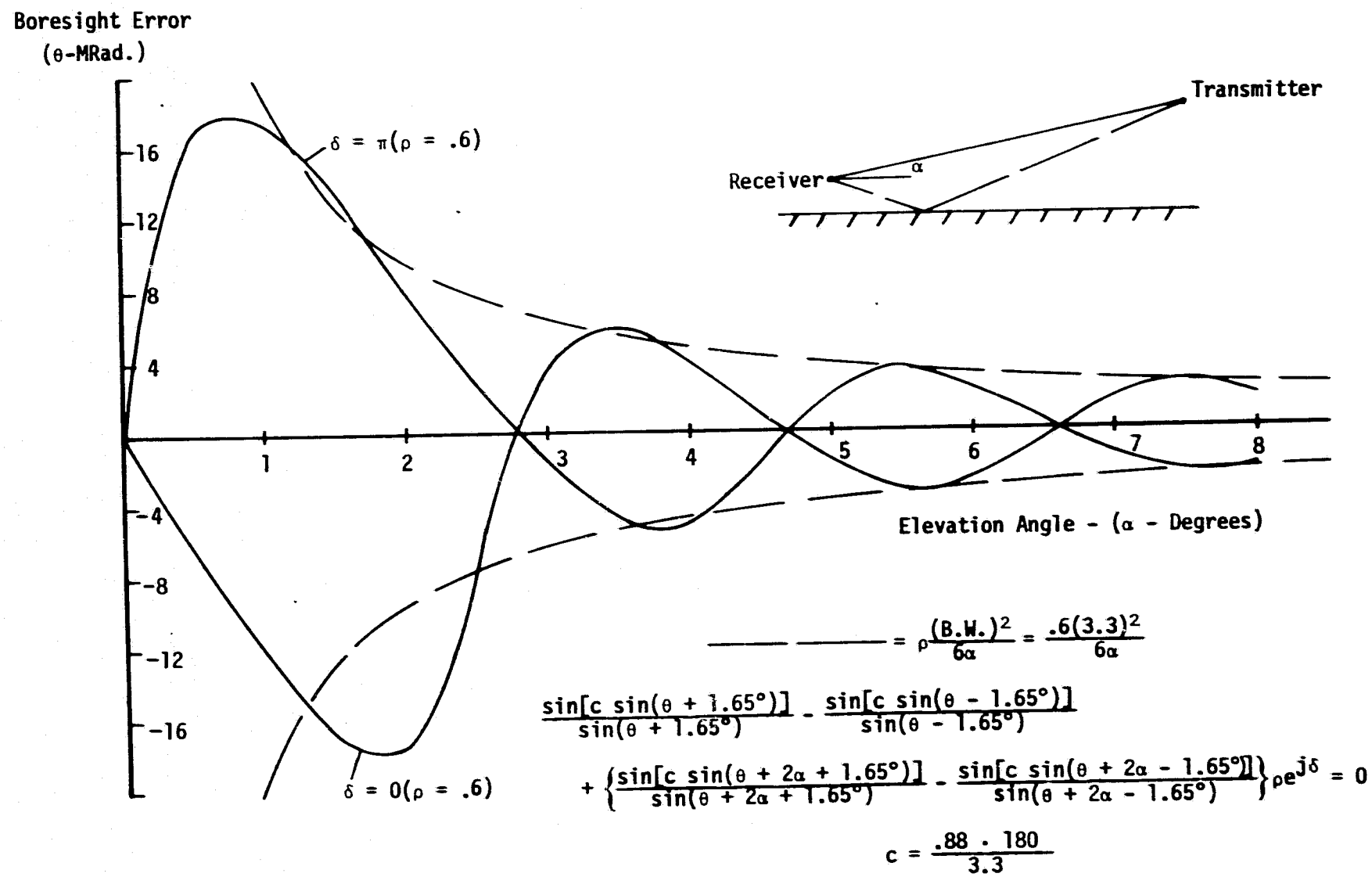

Figure B-1. Solution of Transcendental Equation for Amplitude of Oscillation Due to Multipath

The ground reflection coefficient ρ was set equal to .6 since the relative dielectric constant at the White Sands Missile Range was estimated to be approximately 3 and the conductivity was considered negligible at the operating frequency of the Rendezvous Radar [6].

An approximate expression can be used to estimate the amount of boresight error due to multipath and is represented by the dashed lines in Figure B-1 [5,7]. This expression can normally be used when the elevation angle is equal to or greater than the Rendezvous Radar beamwidth and for a portion less than the beamwidth. For elevation angles less than about 2.75° the maximum boresight error should be determined from the solid curves which are the exact solution for multipath boresight errors of a narrow beam amplitude monopulse antenna system.

APPENDIX C

APPLICATION OF MULTIPATH PHENOMENON TO LUNAR MISSION

During the ascent phase of the lunar mission with the CSM in a 60 n.mi. orbit and the LM in a 10 n.mi. orbit large line-of-sight (LOS) separations will occur. LOS separations of 350 n.mi. to 500 n.mi. will occur in the coast phase of the lunar rendezvous. The shorter range occurs for a nominal lift-off time and the long range for a late lift-off. It is of interest to determine if the multipath phenomenon will be an important effect at these ranges.

Figure C-1 shows that multipath could indeed shift the boresight error beyond the existing 4 milliradian, 3σ specification for angular accuracy at these ranges. At the end of the launch window with a grazing angle (ψ) of 0.795 degrees, a maximum boresight error of 17.8 milliradians could be incurred.

A more detailed analysis of the effect of multipath on the lunar rendezvous mission is necessary to further refine the above values.

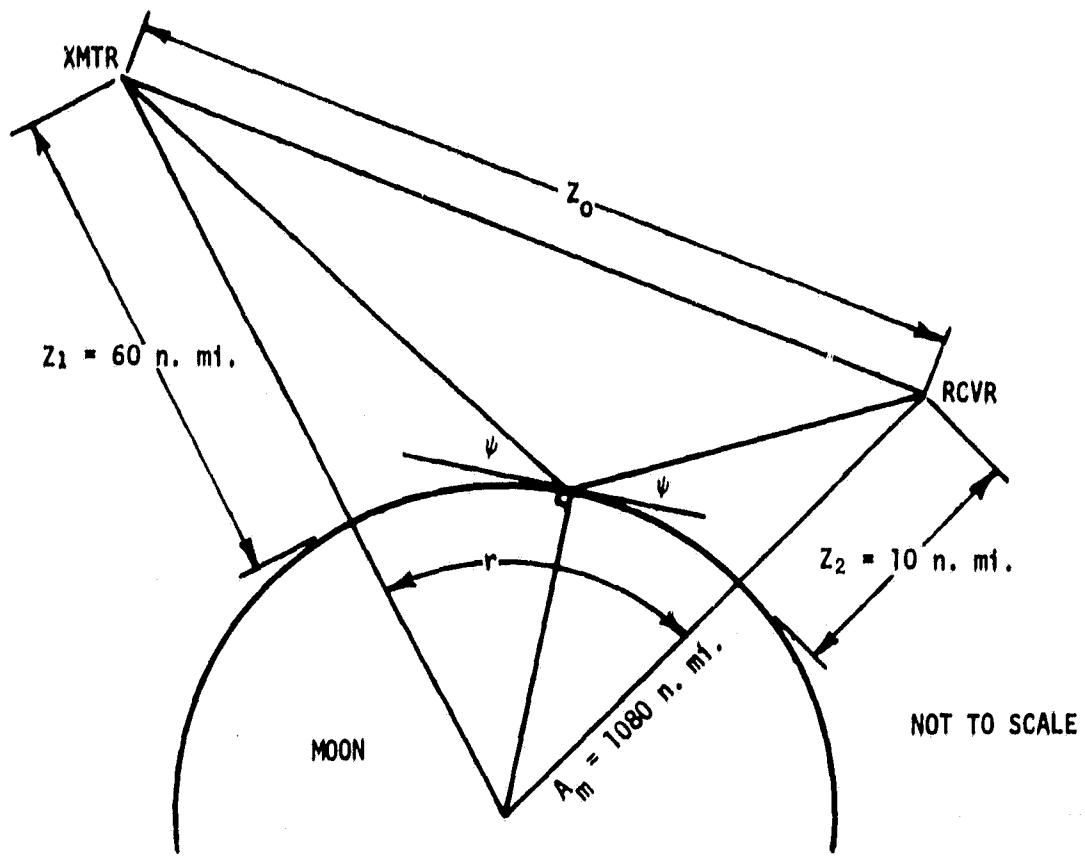

LOS Separation Z_o (n. mi.)	r (n. mi.)	Grazing Angle ψ (Deg)	Max Boresight Error θ (MRAD)
350	322	6.85	2.8
450	430	2.17	15.2
500	475	0.795	17.8

Figure C-1. Lunar Mission Multipath Geometry and Resulting Boresight Error

APPENDIX D

SIGNAL-TO-NOISE VERSUS RANGE FOR RR/T

For reference, curves of received signal-to-noise (S/N) in a 1 KHz bandwidth as a function of range are included in Figures D-1 and D-2.

The (S/N) plotted is at the receiver output and is calculated for the two way transmission by the equation

$$(S/N) = \left[\frac{P_t \, G_{RR} \, G_T \, \lambda^2}{(KT)(B)(\overline{NF})(\Sigma \text{ losses})}\right] \frac{1}{(4\pi R)^2}$$

Maximum, nominal, and minimum values for all parameters but range were taken from the RCA RR/T Power Budget. The (S/N) was then plotted as a function of range for the best, worst, and nominal cases.

Figure D-1 plots (S/N) versus range for ranges between 0 n.mi. and 8 n.mi.

Figure D-2 plots (S/N) versus range for ranges between 0 n.mi. and 400 n.mi.

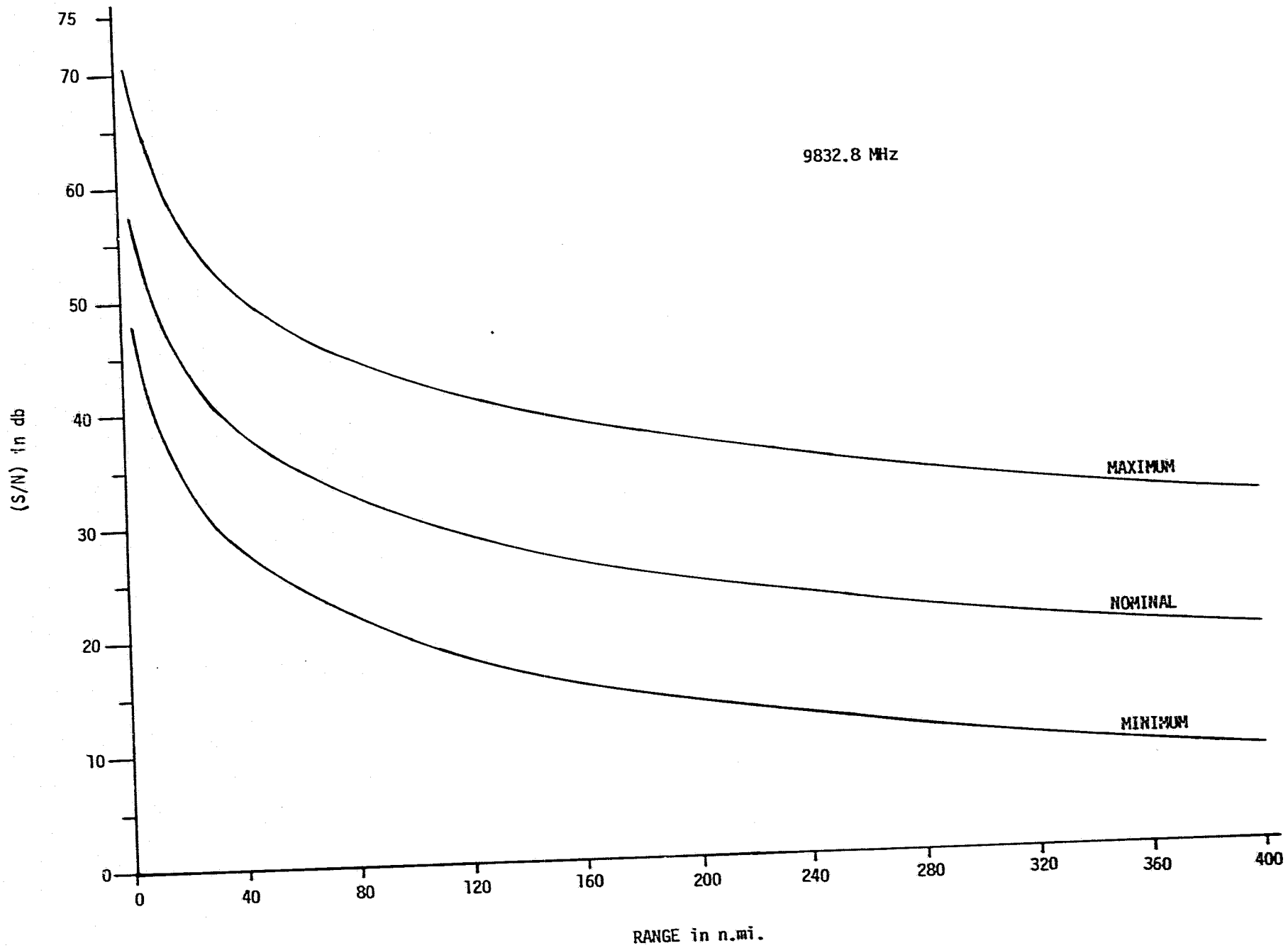

Figure D-1. Received S/N Versus Range Between 0 n.mi. and 8 n.mi. in a 1 KHz Bandwidth

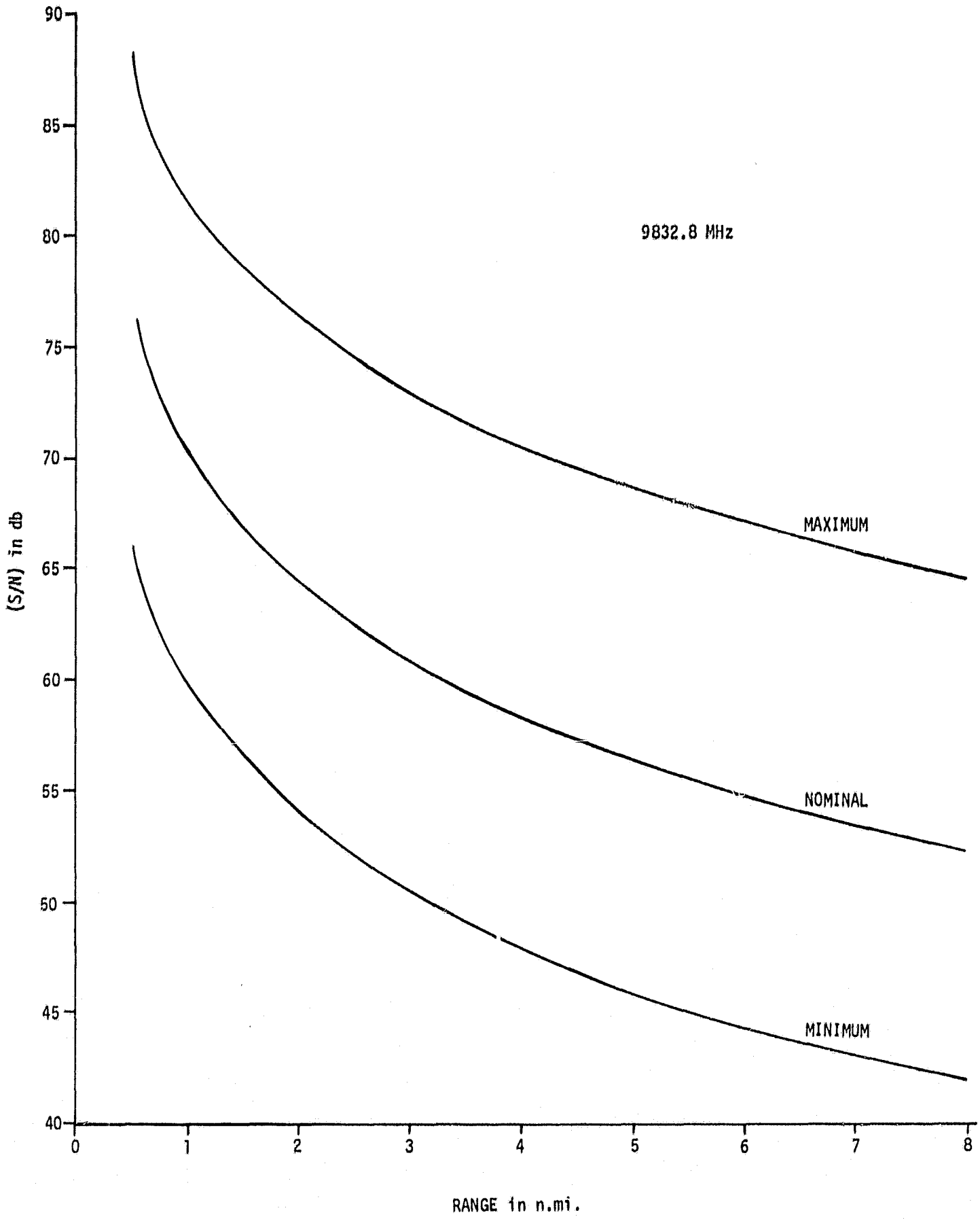

Figure D-2. Received S/N Versus Range Between 0 n.mi. and 400 n.mi. in a 1 KHz Bandwidth

REFERENCES

1. Rendezvous Radar Test Flight Series Notes, White Sands Missile Range.

2. "Lunar Module Test Report for Rendezvous Radar Flight Test at White Sands Missile Range," No. LTR 372-011, September 27, 1968, Grumman Aircraft Engineering Corporation.

3. Pownnell, H. W. and Vallance, A. G., "Quick Look Analysis of Rendezvous Radar Test Flights," Internal Correspondence, RCA.

4. "Minutes of Radar Integration Meeting" L09N - RIM, September 17, 1968, MSC-Houston (Test Document TPS 1205).

5. Evans, G. C., "Influence of Ground Reflections on Radar Target-Tracking Accuracy," Proc. I.E.E. Vol. 113, No. 8, England, August 1966.

6. Sherwood, E. M. and Ginzton, E. L., "Reflection Coefficients of Irregular Terrain at 10 CM," Proceedings of The IRE, July, 1955, pp. 877-878.

7. Shaw, A. H., "An Expression for the Ground Reflection Elevation Error of an Auto-Tracking Radar at Elevations Comparable with the Beamwidth," Royal Radar Establishment, Great Malvern, England, Internal Memorandum 1457.